Impact of the Effective Mass on the Mobility in Si Nanowire Transistors

Cristina Medina-Bailon
School of Engineering
University of Glasgow
Glasgow, United Kingdom
Cristina.MedinaBailon@glasgow.ac.uk

Toufik Sadi
Department of Neuroscience and Biomedical Engineering
Aalto University
Aalto, Finland
toufik.sadi.@aalto.fi

Mihail Nedjalkov
Institute for Microelectronics
TU Wien
Vienna, Austria
mixi@iue.tuwien.ac.at

Jaehyun Lee
School of Engineering
University of Glasgow
Glasgow, United Kingdom
Jaehyun.Lee@glasgow.ac.uk

Salim Berrada
School of Engineering
University of Glasgow
Glasgow, United Kingdom
Salim.Berrada@glasgow.ac.uk

Hamilton Carrillo-Nunez
School of Engineering
University of Glasgow
Glasgow, United Kingdom
Hamilton.Carrillo-Nunez@glasgow.ac.uk

Vihar P. Georgiev
School of Engineering
University of Glasgow
Glasgow, United Kingdom
Vihar.Georgiev@glasgow.ac.uk

Siegfried Selberherr
Institute for Microelectronics
TU Wien
Vienna, Austria
selberherr@iue.tuwien.ac.at

Asen Asenov
School of Engineering
University of Glasgow
Glasgow, United Kingdom
Asen.Asenov@glasgow.ac.uk

***Abstract*— In the simulation based research of aggressively scaled CMOS transistors, it is mandatory to combine advanced transport simulators and quantum confinement effects with atomistic simulations which accurately reproduce the electronic structure at the nanometer scale. This work investigates the impact of cross-section dependent effective masses, obtained from atomistic simulations, on the mobility in Si nanowire transistors (NWTs). For the transport simulations, we use the Kubo-Greenwood formalism with a set of multisubband phonon, surface roughness, and impurity scattering mechanisms.**

Keywords*— *Transport Effective Mass; Phonon Scattering; Surface Roughness Scattering; Impurity Scattering; Kubo-Greenwood Formalism; Matthiessen rule; Nanowire FETs

I. Introduction

In the nanodevice transport simulation framework, approaches which incorporate important quantum effects into semi-classical models have become very popular due to their lower computational cost in comparison to the purely quantum transport simulation techniques. Therefore, their application to simulate nanowire transistors (NWTs), which are considered as candidates to replace FinFETs in the future CMOS technology nodes, remains of a continuing interest. The low-field electron mobility is one of the parameters which determines the NWTs performance [1]. In addition, silicon NWTs do not have bulk-like electronic structure for diameters smaller than 8nm [2]. Accordingly, any realistic electronic structure model must accurately reproduce the experimental energy gaps and effective masses for the most relevant subbands.

This work was supported by the European Union's Horizon 2020 research and innovation programme under grant agreement No 688101 SUPERAID7. The authors would like to thank Dr. Ewan Towie for useful discussions.

The strategy considered herein combines: *(i)* extracting and calibrating the effective masses of the NWTs from atomistic simulations; *(ii)* accounting for quantum effects based on the rates of the relevant multisubband scattering mechanisms in NWTs [3]; and *(iii)* using the semi-classical Boltzmann transport equation (BTE) in the relaxation time approximation by adopting the Kubo-Greenwood formalism [5]-[6]. This framework provides reliable mobility values at low-field near-equilibrium conditions in devices with strong confinement effects, such as NWTs.

The aim of this work is to perform a simulation study of the impact of the effective masses on the electron mobility in silicon NWTs as a function of nanowire size and geometry, comparing the use of bulk effective masses and effective masses extracted from atomistic electronic structure simulations. For this purpose, in Section II, a detailed discussion of the mobility simulation approach is provided, together with the details of the considered scattering mechanisms. The main findings from the simulations are reported in Section III, including a meticulous analysis of the impact of the effective mass choice on the total mobility as a function of size and geometry. Finally, conclusions are given in Section IV.

II. Methodology

The assumption herein considered for the mobility calculation, using the relaxation time approach, is based on the long-channel simulation model. Its capabilities have already been shown by studying the impact of the different scattering mechanisms and the cross-section dimensions on the NWT

performance [7]-[8]. The innovation in this work is the pre-calculation of the effective masses (m_{eff}) from atomistic simulations, instead of using the bulk (m_{bulk}) ones. The effective masses are extracted from $sp^3d^5s^*$ tight-binding simulations with a Boykin parameter set [9].

Different steps are included in the aforementioned approach. Firstly, multiple cross sections of the device (Fig.1) are simulated taking into account the calibrated effective masses and applying a low constant electric field in the transport direction. In this particular work, the coupled 3D Poisson and 2D Schrödinger solver integrated in the TCAD simulator GARAND from Synopsys [10] has been used to pre-calculate the required potential distribution and the corresponding values and eigenfunctions.

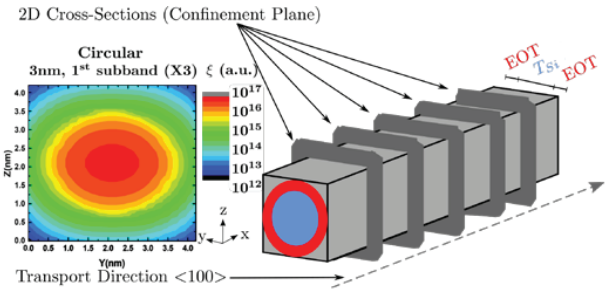

Fig. 1. NWT structures analyzed in this work with widths ranging from 3nm to 8nm. The coupled 3D Poisson and 2D Schrödinger equation are solved for each cross-section (confinement plane). The scattering rates are then calculated accounting for the potential and the eigenfunctions for each subband.

Secondly, the calibrated transport effective masses, the potential distribution, and the corresponding eigenfunctions are included in the multisubband scattering rates, whose expressions have been directly derived based on the Fermi's Golden Rule, accounting for the multisubband quantization in the NWT plane of confinement. These scattering mechanisms redistribute the electron concentrations between different subbands.

The following scattering mechanisms have been incorporated in this study: *(i)* acoustic phonon scattering; *(ii)* optical phonon scattering (with fixed parameters for the different branches); *(iii)* surface roughness scattering; and *(iv)* ionized impurity scattering, with a constant effective ionized impurity concentration $n_0=10^{18}cm^{-3}$. In general, phonon scattering is a strong mobility limiting mechanism in Si NWTs, because it is intrinsic to the material. Nevertheless, we have also focused our attention on the surface roughness and ionized impurity scattering mechanisms due to their dependence on the device geometry and environment. The models for electron interactions with phonons (acoustic and optical) and impurities have been already described in Ref. [7], whereas the inclusion of the surface roughness scattering mechanism is the second innovation in this work. It plays an important role especially at high charge densities in realistic devices with strong confinement effects, where the electrons remain close to the non-ideal surfaces. This model directly depends on the force normal to the interface, which is represented as the interaction of the wavefunctions with the electric field, and the statistics given by the root mean square (Δ_{RMS}) and correlation length [1]. In this work, Δ_{RMS} and the correlation length have been considered as 0.50nm and 1.5nm, respectively.

Thirdly, the mobility associated with each particular scattering mechanism is calculated using its rate by applying the Kubo-Greenwood formula to the relaxation time approach. Finally, the total mobility is calculated as a function of the individual mobilities associated with each scattering mechanism using the Matthiessen rule [11].

Following this assumption, the effect of the dimension on the effective masses is included in each device by using the calibrated effective masses in the Poisson-Schrödinger solver and also incorporating the transport effective masses in each scattering rate. By doing so, the band structure is reproduced for each NWT's configuration. Furthermore, the advantage of this combined semi-classical strategy in comparison with purely quantum transport is that it allows the computation of each mechanism separately reducing substantially the total simulation time.

III. Results and Dicussion

Fig.1 shows the device parameters for the silicon gate-all-around (GAA) NWTs herein analyzed. The nanowire thickness and width range from 3nm to 8nm in both square and circular cross-sectional shapes. The gate equivalent oxide thickness (EOT) is 0.8nm for all the dimensions, whereas the gate bias is adjusted to obtain the sheet density reported in the following results. Despite the fact that both square and circular shapes are studied in the [100] transport direction, we have considered a 3nm circular NWT for the initial effective mass comparison due to the stronger confinement impact [7] and mobile charge [12]. In addition, the difference between m_{bulk} and m_{eff} is higher for the smallest NWT dimension as can be seen in Fig.2, which shows the deviation in % of the longitudinal (m_l) and transverse (m_t) effective masses as a function of the cross-sectional area, for both square and circular NWTs. The deviation is estimated by the modulus of the difference between m_{bulk} and m_{eff} and then divided by m_{eff}. The difference is more pronounced in the transport effective mass m_t which corresponds to the most populated valley (X3), and so it will dominate the changes between both simulations.

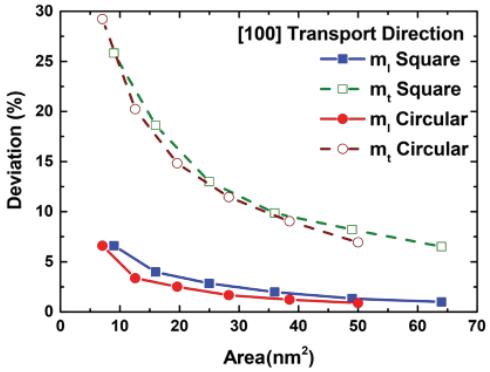

Fig. 2. Deviation (%) of the longitudinal (m_l) and transverse (m_t) effective masses as a function of the cross-sectional area for both square and circular NWTs and [100] orientation.

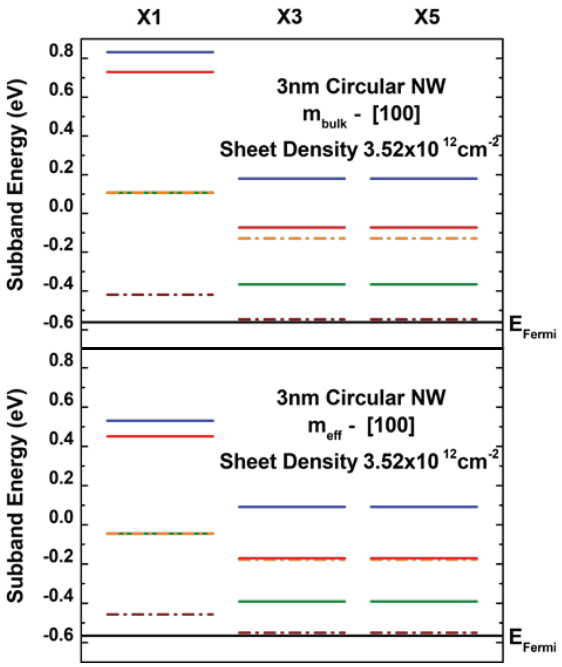

Fig. 3. Energy levels for a 3nm circular NW with m_{bulk} (top) and m_{eff} (bottom) masses and a sheet density of $3.2x10^{12}cm^{-2}$, showing band splitting for the set of valleys X1, X3, and X5.

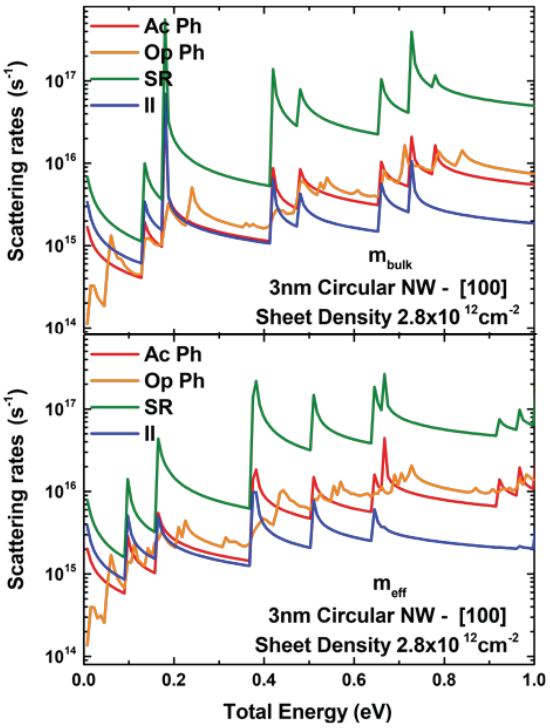

Fig. 4. Acoustic (Ac Ph) and optical (Op Ph) phonon, surface roughnes (SR), and ionized impurity (II) scattering rates as a function of the total energy for a 3nm circular NW with m_{bulk} (top) and m_{eff} (bottom) masses and a sheet density of $3.52x10^{12}cm^{-2}$.

Fig.3 presents the energy levels for the 3nm circular NWT with m_{bulk} (top) and m_{eff} (bottom). The difference between the lower and upper subbands with m_{eff} is smaller than the other. It means that the possible electron transitions between subbands increases when m_{eff} is taken into account. Following this reasoning, the multisubband effects would be less pronounced considering confinement m_{eff} and so the electron mobility would be higher ($\mu_{eff}>\mu_{bulk}$). However, the electron mobility is inversely proportional to the transport effective mass and so the larger m_{eff} in comparison to m_{bulk} (Fig.2) reduces the mobility ($\mu_{eff}<\mu_{bulk}$). Let us elaborate this at first glance contradictory fact. Fig.4 presents the scattering rates for a 3nm circular NWT with m_{bulk} (top) and m_{eff} (bottom) as a function of the total energy of electrons considering acoustic phonon, optical phonon, surface roughness, and ionized impurity scatterings. We have taken 20 subbands into account for this calculation. In general, the scattering rates are proportional to the transport effective mass and so the increase m_{eff} in comparison to m_{bulk} increases the rates. Due to the relaxation time approach, the mobility for a particular scattering mechanism is inversely proportional to its rate. Accordingly, there is a reduction of the mobility, when m_{eff} is included in the scatering rate, as depicted in Fig.5. This figure shows the electron mobility as a function of the sheet density for each mechanism separately as well as the combined cases. One can realize that the effect of the m_{eff} decreases both, the individual and the total mobililities.

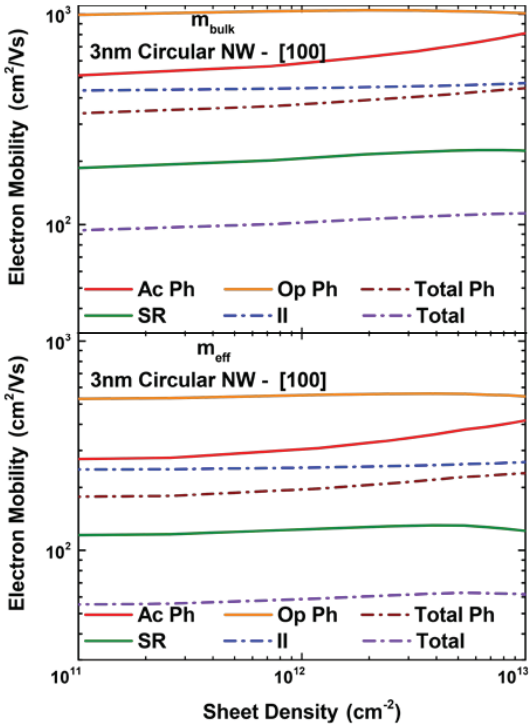

Fig. 5. Electron mobility as a function of the sheet density considering acoustic (Ac Ph), optical (Op Ph), total phonon (Total Ph), surface roughness (SR), and ionized impurity (II) scattering separately, as well as the combined mechanisms, for a 3nm circular NW with m_{bulk} (top) and m_{eff} (bottom) masses.

Finally, Fig.6 shows the total mobility (including acoustic and optical phonon, surface roughness, and ionized impurity scattering) of square and circular NWTs as a function of the cross-section area for both effective masses. As expected, the difference between both effective masses is more pronounced for small cross-section devices. Moreover, the decrease of the mobility in the circular NTWs is more pronounced, because the deviation in m_t is higher in this shape (Fig.2).

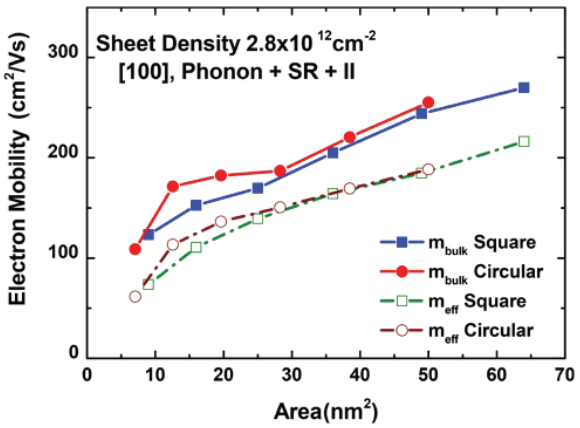

Fig. 6. Total electron mobility as a function of the area for a square and circular NW with a sheet density of $3.52x10^{12}cm^{-2}$. The acoustic and optical phonon, surface roughness, and ionized impurity scattering mechanisms are being included in order to calculate the total electron mobility.

IV. Conclusions

This work presented a simulation study of the impact of the effective mass on the electron mobility in silicon NWTs as a function of the nanowire size and geometry. The focus was on comparing the use of bulk effective masses and effective masses extracted from first principle electronic structure calculations. The Kubo-Greenwood formalism has been herein considered, which makes use of the relaxation time approximation of a 1D electron gas by combining the semi-classical Boltzmann transport equation with quantum effects. The quantum effects are described by the rates of the most relevant scattering mechanisms, which for this work include: phonon (acoustic and optical), surface roughness, and ionized impurity. We have demonstrated that the use of transport effective mass extracted from atomistic simulations, as a function of its cross-section for each device, is not negligible. Therefore this approach becomes mandatory as the NWT dimensions are scaled down. Moreover, as the scattering rates are proportional to the transport effective masses, the change in these masses is most relevant, and will dominate the difference between both simulations. Finally and for these particular devices, the change of the mobility in the circular NWTs is more pronounced because the deviation in m_t (the transport effective mass) is higher for this cross-sectional shape.

References

[1] I. M. Tienda-Luna, F. G. Ruiz, A. Godoy, B. Biel, and F. Gámiz, "Surface roughness scattering model for arbitrarily oriented silicon nanowires," Journal of Applied Physics, vol. 110, no. 8, p. 084514, 2011.

[2] Z. Stanojević, O. Baumgartner, V. Sverdlov, and H. Kosina, "Electric band structure modeling in strained Si-nanowires: Two band k·p versus tight binding," International Workshop on Computational Electronis (IWCE), pp.1-4, October 2010.

[3] S. Jin, M. V. Fischetti, and T.-W. Tang, "Modeling of electron mobility in gated silicon nanowires at room temperature: surface roughness scattering, dielectric screening, and band nonparabolicity," J. Appl. Physics, vol. 102, no. 8, p. 083715, 2007.

[4] L.S.D. Esseni and P. Palestri, "Nanoscale MOS transistors: Semi-classical transport and applications," Cambridge University Press, 2011.

[5] D. Ferry and C. Jacobini, "Quantum transport in semiconductors," Springer Science, 1992.

[6] S. Jin, T.W. Tang, and M. V. Fischetti, "Simulation of silicon nanowire transistors using Bolzmann transport equation under relaxation time approximation," IEEE Trans. Elec. Dev., vol. 55, no. 3, pp. 727–736, 2008.

[7] C. Medina-Bailón et al., "Study of the 1D scattering mechanisms' impact on the mobility in Si nanowire transistors," EUROSOI workshop and international conference on Ultimate Integration on Silicon (EUROSOI-ULIS), pp.1-4, March 2018.

[8] S. Berrada, H. Carrillo-Nuñez, J. Lee, C. Medina-Bailon, T. Dutta, M. Duan, F. Adamu-Lema, V. Georgiev, and A. Asenov, "NESS: new flexible Nano-Electronic Simulation Software," in Proc. SISPAD 2018.

[9] T.B. Boykin, G. Kilmeck, and F. Oyafuso, "Valence band effective-mass expresions in the $sp^3d^5s^*$ empirical tight-binding model applied to a Si and Ge parametrization," Physical Review B, vol. 69, no. 11, pp. 115201, 2004.

[10] Garand User Guide, https://solvnet.synopsys.com, Synopsys, inc., 2017.

[11] D. Esseni and F. Driussi, "A quantitative error analysis of the mobility extraction according to Matthiessen rule in advanced MOS transistors," IEEE Trans. Elec. Dev., vol. 58, no. 8, pp. 2415–2422, 2011.

[12] Y. Wang et al., "Simulation study of yhe impact of quantum confinement on the electrostatically driven performance of n-type nanowire transistors," IEEE Trans. Elec. Dev., vol. 62, no. 10, pp. 3229–3236, 2015.